**Proceedings of the ASME 2015 34th International Conference on Ocean, Offshore and Arctic Engineering**
**OMAE2015**
**May 31-June 5, 2015, St. John's, Newfoundland, Canada**

**OMAE2015-41438**

# EVOLUTION OF THE EXTREME WAVE REGION IN THE NORTH ATLANTIC USING A 23 YEAR HINDCAST

**Sonia Ponce de León***
School of Mathematical Sciences/UCD Earth Institute
University College Dublin
Dublin
Ireland
Email: sonia.poncedeleonalvarez@ucd.ie

**João H. Bettencourt**
School of Mathematical Sciences/UCD Earth Institute
University College Dublin
Dublin
Ireland
Email: joao.bettencourt@ucd.ie

**Joseph Brennan**
School of Mathematical Sciences/UCD Earth Institute
University College Dublin
Dublin
Ireland
Email: joseph.brennan.2@ucdconnect.ie

**Frederic Dias**
School of Mathematical Sciences/UCD Earth Institute
University College Dublin
Dublin
Ireland
Email: frederic.dias@ucd.ie

## ABSTRACT

*The IOWAGA data base for the North Atlantic region was used to identify the region where extreme values of significant wave height are more likely to occur. The IOWAGA database [1] was obtained from the WAVEWATCH III model [2] hindcast using the CFSR (Climate Forecast System Reanalysis) from NOAA [3,4]. The period of the study covers 1990 up to 2012 (23 years). The variability of the significant wave height was assessed by computing return periods for sea storms where the significant wave height exceeds a given threshold. The return periods of sea storms where the $H_s$ exceeds extreme values for the north Atlantic region were computed allowing for the identification of the extreme wave regions which show that extreme waves are more likely to occur in the storm track regions of the tropical and extratropical north Atlantic cyclones.*

*Address all correspondence to this author.

## INTRODUCTION

Extreme sea states are a source of risk for marine structures and operations. These extreme sea states are usually generated by storms that can traverse whole ocean basins and generate high-energy swells that can propagate for thousands of kilometers. Additionally, rogue waves due to modulation instability [5] are a recognized source of extreme waves [6, 7] that needs to be taken into account when designing for operation at sea.

The north Atlantic ocean is regularly traversed by extratropical cyclones and winter low pressure systems originated in the Western part of the basin that can potentially generate dangerous extreme sea states [8–10]. The region where these extreme sea states occur is linked to the tracks of the low pressure systems in the north Atlantic basin. The variability of this storm tracks presents a primary dipole pattern with centers in the extreme northeastern Atlantic and west of Portugal. A strong northeastward extension of the storm tracks causes strong maritime flow giving rise to mild European winters and is primarily associated with low-frequency teleconnections [11]. Future cli-


Copyright © 2015 by ASME

mate projections indicate a poleward migration of northern hemisphere storm tracks, with a distinct increase of storm track density and mean intensities in an area over the British Isles and to the north and west while a decrease in number and intensity is projected in the Mediterranean [12].

Since waves are locally generated by surface winds, their trends should be related. Globally, [13] reported a general trend of increasing values of wind speed and wave height (to a lesser extent) based on a 23-year database of satellite altimeter measurements. In addition, the report showed a greater rate of increase in extreme values of wind speed and wave height. In the North Atlantic, the WASA project [14–18] found an increase in the annual maximum of significant wave height ($H_s$) over the last 40 years in the east of the basin. Results from a 40-year hindcast using kinematically reanalyzed wind fields [19] also show a increase in extremes of winter wave height in the east, closely associated to the North Atlantic Oscillation (NAO) variations.

In the design of maritime structures, one is interested in the return periods of extreme events. The 100-year wave, e.g., would be a wave with height exceeded on average once in a 100 years period. A related concept is the annual exceedance probability which is the probability that a wave will exceed a given threshold in 1 year. In percentage terms, the annual exceedance probability of the p–year wave is simply 100/p.

Based on wind and wave reanalysis data, [20, 21] provided global estimates of 100-year wind speed ($U_{10}$) and $H_s$ return values using the peaks–over–threshold (POT) method. The $H_s$ 100-year return value estimates are higher in the storm tracks of the Northern and Southern Hemispheres and lower in the tropics. Decadal variations in the estimates were found to be significant only in the Northern Hemisphere storm tracks and in the western tropical Pacific. These differences were attributed to the decadal variability in the Northern Hemisphere, especially to the NAO. Interdecadal differences for $U_{10}$ were found to be consistent with those of the $H_s$. Nonetheless, a lack of a clear trend in 100-year return value for $H_s$ was reported by [22], using global altimeter measurements spanning 23 years and the initial distribution method.

An equivalent problem of interest for the engineering of maritime structures is the prediction of waves that exceed a given threshold. The return period of a wave exceeding a given threshold was obtained by [23] and [24, 25] studied the statistical properties of waves in storms. Later, [26, 27] solved the problem of the return period of a sea storm during which the wave height exceeds a given threshold. Thereafter, extensions to the return period of nonlinear high waves, arbitrary number of waves and generalized storm models were presented [28–30].

In this paper, we compute return periods of sea storms where the $H_s$ exceeds extreme values for the north Atlantic region. Using a 23 year wave hindcast database covering the whole North Atlantic, the distribution of return periods in the basin can be computed. The hincast interval is then divided in 4 year periods

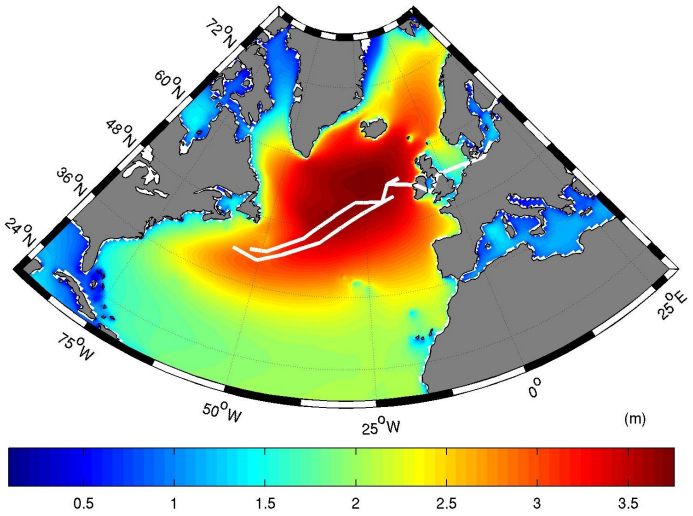


**FIGURE 1**. AVERAGE IOWAGA $H_S$ OVER THE 23-YEAR PERIOD: 1990–2012. WHITE LINES ARE CYCLONE TRACKS FOR FEB 2007 FROM [33].

to observe the evolution of the return period distributions. We use an analytical sea storm model in order to circumvent the necessity of choosing a priori the distribution of extreme $H_s$ values at the peak of the storms.

## DATA AND METHODS

### The IOWAGA hindcast

The IOWAGA data base [1] is a multi-scale global hindcast of ocean waves. The hindcast database is freely available for the period 1990–2012 and it is based on the parameterizations for wind sea and swell dissipation of [31] and forcing from a combination of ECMWF analysis and CFSR reanalyses, sea ice from CFSR and ECMWF and icebergs from CERSAT. From the validation with altimeter and buoy data they concluded that CFSR winds are anomalously high in the Southern Ocean for the years 1991–1993 [32].

The area chosen for this study is the north Atlantic ocean from 90°W to 30°E and 18°N to 80°N (see Fig. 1). The resolution of the return period maps is 0.5° in each direction. The time series of $H_s$ at each grid node location has a time step of 3 hours. For the identification of storms, missing values in the $H_s$ time series were set to zero.

The mean $H_s$ distribution for the 23-year hindcast ( Fig. 1), shows the highest values on the eastern part of the basin in a region extending towards the western boundary where mean $H_s$ values are lower. This area coincides with the northern north Atlantic storm track area.


Copyright © 2015 by ASME

### Equivalent triangular storm

A sea storm is defined as a sequence of sea states where the $H_s$ is above a given threshold $h_p$ for a predefined amount of time. In [27], the threshold $h_p$ is defined as $1.5\bar{H}_s$ with $\bar{H}_s$ the annual mean of $H_s$ and the continuos time period as 12 hours. With these two conditions and given a record of $H_s$ a sequence of storms can be defined for a specific location.

Each of the members of this storm sequence can then be approximated by an analytical function of time that, during the storm duration $b$ gives the $H_s$ as

$$h(t) = a[1-(\frac{2t}{b})], \quad -\frac{b}{2} \leq t \leq \frac{b}{2}, \tag{1}$$

where values of $t < 0$ indicate time before the peak of the storm ($t = 0$). The storm intensity $a$ is the maximum wave height achievable during the storm. The parameters $a$ and $b$ defined the equivalent triangular storm (ETS) model [27, 34].

### Return period of a storm where $H_s$ exceeds a threshold

Considering a series of $N(\tau)$ storms ocurring at a given location during a time interval $\tau$, the time $T_h$ during which $H_s$ stays above a given threshold $h$ is $T_h = \tau P(h)$, where $P(h) = P(H_s > h)$. According to [30], the return period of a storm during which $H_s$ exceeds $h$ can be computed as

$$R_h = \frac{\tau}{N(\tau; H_s > h)}, \tag{2}$$

where $N(\tau; H_s > h)$ is the average number of storms where the $H_s$ exceeds $h$.

The ETS model can be used to compute the return period given by eqn. 2. The method presented by [30] is described: considering that $a$ and $b$ are realizations of the random variables storm intensity $A$ and storm duration $B$, the joint probability density function (pdf) of $A$ and $B$ is defined as $p_{A,B}(a,b) = p_A(a)p_{B|A}(b|a)$ and $p_{A,B}(a,b)dadb$ as the number of equivalent storms with intensity between $(a, a+da)$ and duration between $(b, b+db)$. The pdf of $A$ is then

$$p_A(a) = \int_0^\infty p_{A,B}(a,b)db, \tag{3}$$

and the number of equivalent storms having intensity between $(a, a+da)$ and duration between $(b, b+db)$ is

$$dN(a,b) = N(\tau)p_A(a)p_{B|A}(b|a)dadb, \tag{4}$$

from which the average number of equivalent storms with $A > h$ can be computed as

$$N(\tau; A > h) = \int_{a=h}^\infty \int_0^\infty dN(a,b) = N(\tau) \int_{a=h}^\infty p_A(a)da. \tag{5}$$

The return period can then be obtained by replacing $N(\tau; A > h)$ in eqn. 2. The storm intensity pdf is given by [30]

$$p_A(a) = \frac{\tau}{N(\tau)} \frac{a}{\bar{b}(a)} G(\lambda, a), \tag{6}$$

where $\bar{b}(a)$ is the conditional average duration of B given $A = a$. The function $G(\lambda, a)$ is given for the case of the ETS, by:

$$G(\lambda, a) = \frac{d^2P}{da^2}, \tag{7}$$

with $P(h) = P(H_s > h)$.

To compute the conditional average duration $\bar{b}(a)$ for a given $a$, it is approximated by a regression $\bar{b}(a) = K_1 \log(a) + K_2$. To obtain the regression coefficients, we construct a random sequence of $(a,b)$ pairs using the actual storm sequence at the location of interest. The storm intensity $a$ is the maximum $H_s$ for each storm and the duration is found by requiring that the expected maximum wave height $\bar{H}_{max}$ is the same for the actual and for the equivalent storm.

### Computation of exceedance probability $P(H_s > h)$

We assume that the exceedance probability of the $H_s$ is given by a lower-bounded three parameter Weibull distribution

$$P(h) = 1 - \exp[-(\frac{h-h_l}{w})^u], \quad h \geq h_l, \tag{8}$$

where the unknown parameters are obtained by least-squares fitting to the $H_s$ time series. This method allows to obtain two of the three parameters of the Weibull distribution (eqn. 8), namely the scale parameter $w$ and the location parameter $h_l$. The third parameter, the shape parameter $u$, is chosen as the one that minimizes the residue of the correlation between the fitted distribution and the original data. While the Weibull distribution may fail to represent well the whole distribution, it can fit the low probability part reasonably well [35].

For this reason we have focused our analysis on thresholds above the $99^{th}$ percentile of the $H_s$ exceedance distribution, computed from the Weibull distribution parameters fitted at each data point and shown in Fig.2. The sharp gradients in the map are due to the fact that minimization of the correlation residue between


Copyright © 2015 by ASME

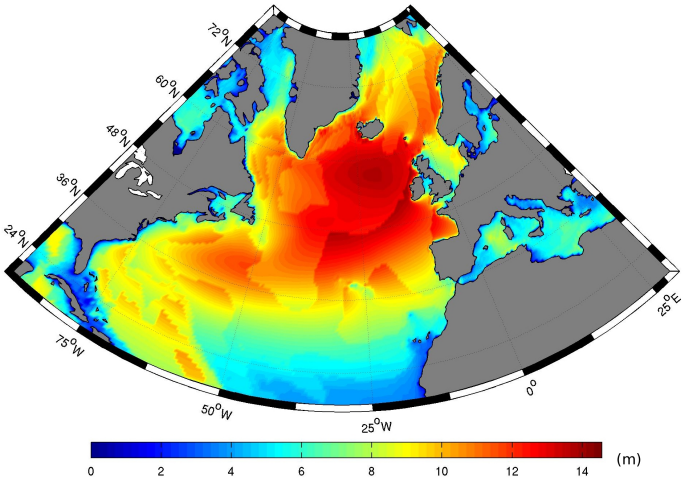


**FIGURE 2**. SPATIAL DISTRIBUTION OF THE $99^{TH}$ PERCENTILE FOR THE $H_S$ IN THE PERIOD: 1990–2012.

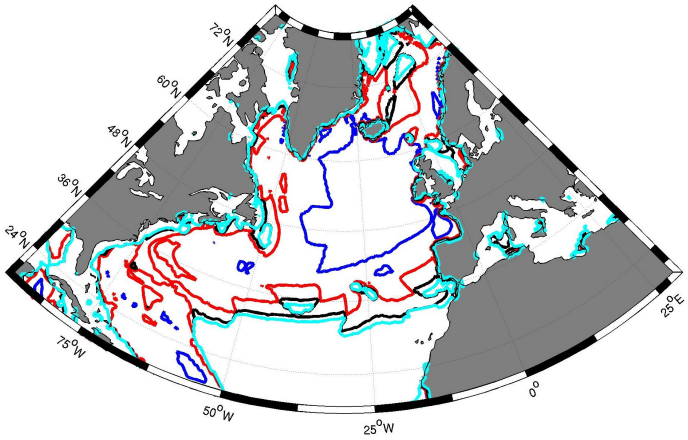


**FIGURE 3**. RETURN PERIODS FOR $H_S > 20$ M. LINES ENCLOSE REGIONS WHERE RETURN PERIOD IS LESS THAN 1 YEAR (BLUE); 10 YEARS (RED); 50 YEARS (BLACK); 100 YEARS (CYAN).

the fitted distribution and the original data, was performed by direct search over a discrete set of values of $u$, between 0.75 and 2.0. Due to the computationally expensive nature of this process for the amount of grid points, only 15 values of $u$ were used between these limits and thus sharp changes in the $u$ distribution were obtained, which were reflected in the $99^{th}$ percentile distribution.

## RESULTS

### Return periods for the 23-year hindcast

The return periods of sea storms where the $H_s$ exceeds a given threshold were computed for several $H_s$ values in North Atlantic.

In Fig. 3 the return period contours for the $H_s$ threshold of 20 m are shown. At the 1-year return period level of sea storms, the contours delimit the eastern north Atlantic from 40°N to Iceland, the bay of Biscay and several small scale regions in the Caribbean and Atlantic. At the 10-year level, the region is enlarged to the whole north Atlantic northward from 30-36°N, a portion of the western Atlantic below these latitudes, roughly between 50 and 75°W and two small regions in the Gulf of Mexico and in the Caribbean sea. At the 50 and 100 years return period level, the contours practically coincide and limit a region combining the two previous ones mentioned for the 10-year return period.

At the 10-year return period level for a sea storm with $H_s$ >20 m, the northern Atlantic region matches well with the storm track region of north Atlantic cyclones [36], while the western Atlantic region below 30 °N, the Gulf of Mexico and Caribbean sea corresponds to the north Atlantic tropical cyclone paths. At the 1-year sea storm return period level for the same $H_s$ threshold, the region is greatly reduced to the eastern North Atlantic in the region with the highest 100-year return values of $H_s$, already identified in [20] and [13].

### Evolution of the extreme wave region

To study the evolution of the extreme wave region, the 23 year hindcast was divided in five 4 year periods, starting in 1992. In order not to split the winters between differents years, the beginning and end of year were set at $1^{st}$ of July and $30^{th}$ of June, respectively. In Fig. 4, the return period for sea storms with $H_s$ threshold set at 25 m is shown for the periods 1992–1996 (top panel) and 1996–2000 (bottom panel). The major difference was found between the 1996–2000 period and the others, where a decrease in the area delimited by the 50 and 100 years return period contours was found. This coincides with a jump in the reanalysis winds particularly visible in the $99^{th}$ percentile winds [32]. The $99^{th}$ percentile has a significant impact on wave height in the wave model when modelling extreme events such as hurricanes.The remaining periods (2000–2004, 2004–2008, 2008–2012) have return period distributions very similar to the 1992–1996 period.

The reduction in area observed in the 1996–2000 period is not completely clear as to its reasons but the uses of different data assimilation techniques and inconsistent reanalysis could be the causes [37]. Also, The 5 year period between 1995-2000 was characterized by a multi–decadal increase in sea surface temperature and an increase in the number of Atlantic major hurricanes [38]. On the other hand, no clear tendency in increase or reduction of the extreme wave region could be identified in the whole period, in agreement with the lack of tendency for the 100-year $H_s$ return values found by [22].


Copyright © 2015 by ASME

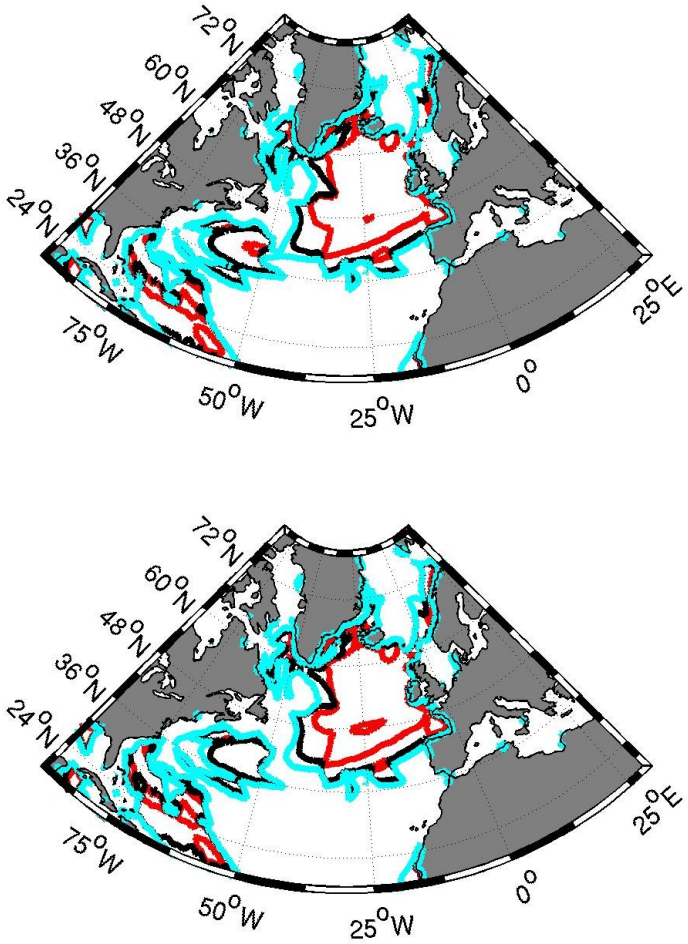


**FIGURE 4**. RETURN PERIODS FOR $H_S > 25$ M. TOP PANEL: 1992-1996; BOTTOM PANEL: 1996-2000; LINE COLOURING AS IN FIG.3

## CONCLUSIONS

The extreme wave regions of the North Atlantic were identified by computing return periods of sea storms were the $H_s$ exceeds a given threshold. Using a 23-year hindcast of the whole North Atlantic region, spatial distributions of the return periods were obtained.

The return period maps, show that extreme waves are more likely to occur in the storm track regions of the tropical and extratropical north Atlantic. For an $H_s$ threshold of 20 m, return periods of 1 year or less are limited to the eastern North Atlantic zone above 40°N. It was not possible to observe any trend in the return period values through the time period considered, but a decrease in the 25 m sea storm return period was found for the period of 1996–2004. The reason for this reduction is not completely clear and further analysis is needed to clarify this.

The return period estimates based on equivalent storm models presented in this paper appear to be conservative when compared to $H_s$ return values, e.g. [22] reports a 100-year $H_s$ return level of 26 m for the north Atlantic region whereas in this study the return period of a storm where $H_s > 25$ m can be lower than 50 years. Computations based on the POT method at selected locations (not shown) also show higher return periods for the same $H_s$ level using the ETS model. Other source of error in this work is the extrapolation (implicit in the choice of the $H_s$ threshold) for values of return period much larger than the length of available records (measured or hindcasted by models). This procedure is justified by the need to work with conservative load levels in the process of engineering design of marine structures.

To conclude, the ETS provides a valuable tool to compute design values of wave loads. By using the ETS model of [27], it was not necessary to impose a distribution type to the distribution of $H_s$ storm peaks. Further work is being done to improve certain aspects of the computation and application to other ocean basins is being planned.

## ACKNOWLEDGMENT

This work is based upon works supported by the European Research Council (ERC) under the research project ERC-2011-AdG 290562-MULTIWAVE and Science Foundation Ireland under grant number SFI/12/ERC/E2227.

## REFERENCES

[1] Rascle, N., and Ardhuin, F., 2013. "A global wave parameter database for geophysical applications. Part 2: Model validation with improved source term parameterization". *Ocean Modelling,* ***70***, pp. 174–188.

[2] Tolman, H. L., and Group, D., 2014. User manual and system documentation of WAVEWATCH III version 4.18. Tech. Rep. Tech. Note 316, NOAA/NWS/NCEP/MMAB.

[3] Saha, S., Moorthi, S., Pan, H.-L., Wu, X., Wang, J., Nadiga, S., Tripp, P., Kistler, R., Woollen, J., Behringer, D., et al., 2010. "The NCEP climate forecast system reanalysis". *Bulletin of the American Meteorological Society,* ***91***(8), pp. 1015–1057.

[4] Saha, S., Moorthi, S., Wu, X., Wang, J., Nadiga, S., Tripp, P., Behringer, D., Hou, Y., Chuang, H., Iredell, M., Ek, M., Meng, J., Yang, R., Mendez, M., van den Dool, H., Zhang, Q., Wang, W., Chen, M., and Becker, E., 2014. "The NCEP climate forecast system version 2". *Journal of Climate,* ***27***(8), pp. 2185–2208.

[5] Onorato, M., Residori, S., Bortolozz, U., Montina, A., and Arecchi, F., 2013. "Rogue waves and their generating mechanisms in different physical contexts.". *Physics Reports,* ***528***, pp. 47–89.

[6] Viotti, C., and Dias, F., 2014. "Extreme waves induced by strong depth transitions: Fully nonlinear results". *Physics of Fluids,* ***26***(5), p. 051705.


Copyright © 2015 by ASME

[7] OḂrien, L., Dudley, J. M., and Dias, F., 2013. "Extreme wave events in Ireland: 14 680 BP-2012". *Natural Hazards and Earth System Sciences,* ***13***, pp. 625–648.

[8] Shimura, T., Mori, N., and Mase, H., 2013. "Ocean waves and teleconnection patterns in the northern hemisphere". *Journal of Climate,* ***26***(21), pp. 8654–8670.

[9] Ponce de León, S., and Guedes Soares, C., 2014. "Extreme wave parameters under north atlantic extratropical cyclones". *Ocean Modelling,* ***81***, pp. 78–88.

[10] Ponce de León, S., and Guedes Soares, C., 2015. "Hindcast of extreme sea states in north atlantic extratropical storms". *Ocean Dynamics,* ***65***, pp. 241–254.

[11] Rogers, J. C., 1997. "North Atlantic storm track variability and its association to the north Atlantic oscillation and climate variability of northern Europe". *Journal of Climate,* ***10***(7), pp. 1635–1647.

[12] Bengtsson, L., Hodges, K. I., and Roeckner, E., 2006. "Storm tracks and climate change". *Journal of Climate,* ***19***(15), pp. 3518–3543.

[13] Young, I., Zieger, S., and Babanin, A., 2011. "Global trends in wind speed and wave height". *Science,* ***332***(6028), pp. 451–455.

[14] Günther, H., Rosenthal, W., Stawarz, M., Carretero, J., Gomez, M., Lozano, I., Serrano, O., and Reistad, M., 1998. "The wave climate of the northeast atlantic over the period 1955-1994: The wasa hindcast". *Global Atmosphere Ocean System,* ***6***, pp. 121–163.

[15] Bouws, E., Jannink, D., and Komen, G. J., 1996. "The increasing wave height in the north atlantic ocean". *Bull. Am. Meteorol. Soc.,* ***77(10)***, pp. 2275–2277.

[16] Gulev, S., and Hasse, L., 1998. "North atlantic wind waves and wind stress fields from voluntary observing ship data". *Journal of Physical Oceanography,* ***28***, pp. 1107–1130.

[17] Sterl, A., Komen, G. J., and Cotton, P. D., 1998. "Fifteen years of global wave hindcasts using winds from the european centre for medium-range weather forecasts reanalysis: Validating the reanalyzed winds and assessing the wave climate". *Journal of Geohysical Research,* ***103(C3)***, pp. 5477–5492.

[18] Neu, H. J. A., 1984. "Interannual variations and longer-term changes in the sea state of the north atlantic from 1970 to 1982". *Journal of Geophysical Research,* ***89(C4)***, pp. 6397–6402.

[19] Wang, X. L., and Swail, V. R., 2002. "Trends of Atlantic wave extremes as simulated in a 40-yr wave hindcast using kinematically reanalyzed wind fields". *Journal of climate,* ***15***(9), pp. 1020–1035.

[20] Caires, S., and Sterl, A., 2005. "100-year return value estimates for ocean wind speed and significant wave height from the ERA-40 data". *Journal of Climate,* ***18***(7), pp. 1032–1048.

[21] Vinoth, J., and Young, I. R., 2011. "Global estimates of extreme wind speed and wave height". *Journal of Climate,* ***24***, pp. 1647–1665.

[22] Young, I., Vinoth, J., Zieger, S., and Babanin, A., 2012. "Investigation of trends in extreme value wave height and wind speed". *Journal of Geophysical Research: Oceans (1978–2012),* ***117***(C11).

[23] Jasper, N. H., 1956. *Statistical distribution patterns of ocean waves and of wave induced ship stresses and motions with engineering applications*, Vol. 921. Catholic University of America Press.

[24] Borgman, L. E., 1970. "Maximum wave height probabilities for a random number of random intensity storms". *Coastal Engineering Proceedings,* ***1***(12).

[25] Krogstad, H. E., 1985. "Height and period distributions of extreme waves". *Applied Ocean Research,* ***7***(3), pp. 158–165.

[26] Boccotti, P., 1986. "On coastal and offshore structure risk analysis". *Excerpta of the Italian Contributions to the Field of Hydraulic Engineering,* ***1***, pp. 19–36.

[27] Boccotti, P., 2000. *Wave mechanics for ocean engineering*, Vol. 64 of *Oceanography Series*. Elsevier.

[28] Arena, F., and Pavone, D., 2006. "Return period of nonlinear high wave crests". *Journal of Geophysical Research: Oceans (1978–2012),* ***111***(C8).

[29] Arena, F., and Pavone, D., 2009. "A generalized approach for long-term modelling of extreme crest-to-trough wave heights". *Ocean Modelling,* ***26***(3), pp. 217–225.

[30] Fedele, F., and Arena, F., 2010. "Long-term statistics and extreme waves of sea storms". *Journal of Physical Oceanography,* ***40***(5), pp. 1106–1117.

[31] Ardhuin, F., Rogers, E., Babanin, A. V., Filipot, J.-F., Magne, R., Roland, A., Van Der Westhuysen, A., Queffeulou, P., Lefevre, J.-M., Aouf, L., et al., 2010. "Semiempirical dissipation source functions for ocean waves. part i: Definition, calibration, and validation". *Journal of Physical Oceanography,* ***40***(9), pp. 1917–1941.

[32] Chawla, A., Spindler, D. M., and Tolman, H. L., 2013. "Validation of a thirty year wave hindcast using the climate forecast system reanalysis winds". *Ocean Modelling,* ***70***, pp. 189–206.

[33] Serreze, M. C., 2009. Northern hemisphere cyclone locations and characteristics from ncep/ncar reanalysis data. Tech. rep., National Snow and Ice Data Center, Boulder, Colorado USA.

[34] Laface, V., and F, A., 2013. Long-term statistics with equivalent storm models, for extreme values of significant wave height. http://www.ifremer.fr/web-com/metocean-stats-wrkshp/pres/Laface.pdf.

[35] Ferreira, J., and Guedes Soares, C., 2000. "Modelling distributions of significant wave height". *Coastal Engineering,* ***40***(4), pp. 361–374.

[36] Dacre, H. F., and Gray, S. L., 2009. "The spatial distri-

 Copyright © 2015 by ASME

bution and evolution characteristics of north atlantic cyclones". *Monthly Weather Review,* ***137***(1), pp. 99–115.

[37] Dee, D., Uppala, S., Simmons, A., Berrisford, P., Poli, P., Kobayashi, S., Andrae, U., Balmaseda, M. A., Balsamo, G., Bauer, P., Bechtold, P., Beljaars, A., van de Berg, L., Bidlot, J., Bormann, N., Delsol, C., Dragani, R., Fuentes, M., Geer, A., Haimberger, L., Healy, S., Hersbach, H., Hlm, E., Isaksen, L., Kllberg, P., Khler, M., Matricardi, M., McNally, A., Monge-Sanz, B., Morcrette, J., Park, B., Peubey, C., de Rosnay, P., Tavolato, C., Thpaut, J., and F, V., 2011. "The ERA-Interim reanalysis: configuration and performance of the data assimilation system". *Quarterly Journal,* ***137***, pp. 553–597.

[38] Molinari, R. L., and Mestas-Nuñez, A. M., 2003. "North atlantic decadal variability and the formation of tropical storms and hurricanes". *Geophysical research letters,* ***30***(10).



Copyright © 2015 by ASME